

SID



سرویس های ویژه



سرویس ترجمه تخصصی



کارگاه های آموزشی



بلاگ مرکز اطلاعات علمی



عضویت در خبرنامه



فیلم های آموزشی

کارگاه های آموزشی مرکز اطلاعات علمی جهاد دانشگاهی



مباحث پیشرفته یادگیری عمیق؛
شبکه های توجه گرافی
(Graph Attention Networks)



کارگاه آنلاین آموزش استفاده از
وب آو ساینس



کارگاه آنلاین مقاله روزمره انگلیسی

The influence of TiO_2 and Na_2CO_3 on the viscosity and crystallization behavior of mold powders

S. Soltan Attar^{1*}, A. Monshi² and M. Meratian³

Department of Materials Engineering, Isfahan University of Technology, 8415683111, Isfahan, Iran.

Abstract

Mold powders are fluxing agents used as raw materials in the steel industry, which play very important role in processing stability and final surface quality of a product. Surface quality depends particularly on the viscosity and the heat transfer of infiltrated mold flux between the mold wall and the solidified steel shell. Heat flux across the interfacial gap depends on thermal properties of slag layer and its thickness, which is affected by slag properties such as melting, crystallization behavior, and temperature-dependent viscosity. Among all of the components of these powders, fluorine mainly controls the viscosity, solidification temperature and crystallization behavior of mold flux films. However, the volatilization and acidification of the fluoride is a significant health hazard and causes environmental pollution and intensifies the erosion to continuous caster. In this study, TiO_2 is used as a substitution to fluorine in commercial start flux. The substitution possibility was examined by measuring the viscosity and crystallization behavior, when it was compared with the properties of industrial powder. In present study, devitrification has been investigated by DTA non-isothermal experiments. It has been shown that titanium dioxide tends to increase crystallization temperature with increasing the formation of perovskite crystalline phase and this causes a decrease in heat flux between the strand and the copper mold. On the other hand, slag viscosity was decreased with increasing titanium dioxide and Na_2CO_3 content. Further XRD characterizations have provided a similar fraction of crystalline phases through Riaz method in the industrial powder and low fluorine sample with 8wt% TiO_2 .

Keywords: Mold powder, Crystallization, Viscosity, Fluorine.

1. Introduction

Mold powders are fluxing agents used as raw materials in steel industry, which are mainly composed of silicon oxides, aluminum, alkaline and alkali-earth metals, with minor contents of fluorides and carbon¹. Mold powder is added to the free surface of the molten steel so that it is sintered, melted and spread out the molten steel surface. During each oscillation stroke, molten slag is pumped from the meniscus into the gap between steel shell and the copper mold. This slag acts as a lubricant as long as it remains liquid. At this stage, a solid slag layer forms against the mold wall. Depending on the composition and cooling rate of mold slag, the microstructure of multiple formed layers may be glassy, crystalline, or mixtures of both. Fig. 1 shows a 20cm thickness of slag film taken from the corner of an operating caster mold². Among all of the components of these powders, fluoride mainly controls the viscosity, solidification temperature and crystallization behavior of mold flux films. These characteristics directly influence the lubrication and heat transfer of a mold flux film.

** Corresponding author:*

Tel: +98 (912) 1034409, Fax: +98 (311) 3912752

E-mail: s.soltanattar@ma.iut.ac.ir

Address: Department of Materials Engineering, Isfahan University of Technology, 8415683111, Isfahan, Iran.

1. M.Sc.

2. Professor

3. Associate Professor

However, the volatilization and acidification of fluoride is a significant health hazard, so that causes environmental pollution and intensifies the erosion to continuous caster³⁻⁵. Thus decreasing the fluoride content in continuous casting mold fluxes has the great significance.

The heat flux across the interfacial gap depends on the thermal properties of slag layer⁶⁻⁸ and its thickness^{9, 10}, which is affected by slag properties such as melting, crystallization behavior, and temperature-dependent viscosity^{11, 12}. It is reported that the crystalline layer controls heat extraction between the strand and mold wall, although the radiation is very important across glassy and liquid layers. The Crystalline slag with high solidification temperature usually reduces mold heat transfer. This is likely due to lower thermal conductivity of crystalline slag and the thicker solid slag layer that it accompanies the higher solidification temperatures¹³⁻¹⁵. The research of Tylor et al.¹⁶ shows that increasing crystallization ratio of solid mold flux film can decrease the heat flux through the mold and it is conducive to reducing longitudinal cracks of the slab. In the industrial slag containing fluorine, heat transfer is usually controlled by precipitating cuspidine ($3\text{CaO} \cdot 2\text{SiO}_2 \cdot \text{CaF}_2$)¹⁷. But in low-fluoride mold fluxes, there should be another crystal to control heat transfer. Therefore, formation study of crystalline phases in thin mold flux layer is considerable practical interest.

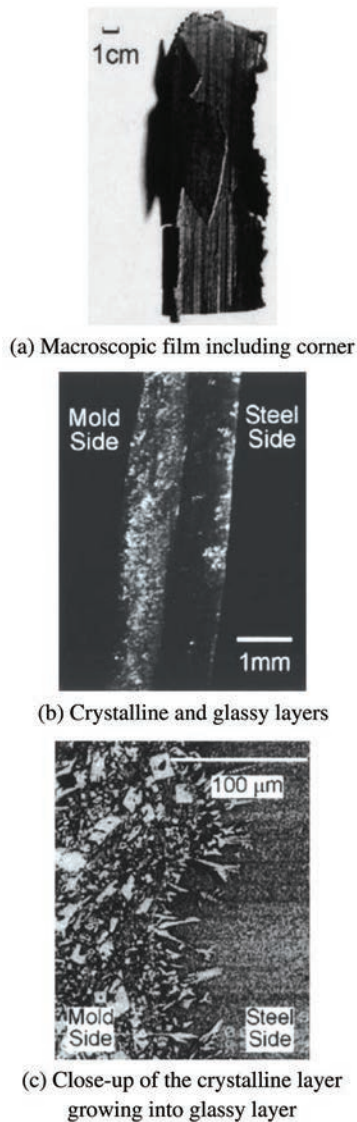


Fig. 1. (a) through; (b) and (c) sample of slag layer and microstructure ²⁾.

The introduction of some new inclusions into the resulting mold powder slag can change its structural properties, as an example in the case of titanium oxide, it tends to increase crystallization temperature, and this causes a decrease in heat flux between the steel and the mold. On the other hand, titanium oxide has a complicated effect on viscosity of mold powder slag. Slag viscosity decreases up to 6wt% with increasing titanium oxide content and then it increases^{3,4)}.

The Common methods were applied to the study of crystallization behavior of mold fluxes range within wide number of techniques. It is preferable to measure crystallization heat using DTA or DSC by isothermal and/or non-isothermal experiments. In previous works, it has been discussed the construction of CCT¹ section of curves with DTA measurements for mold flux slag samples ¹⁸⁻²⁰⁾.

¹Continuous Cooling Transformation diagram (CCT)

In this research, TiO₂ was used as a substitution to the fluorine in commercial start flux. The substitution possibility was examined by measuring the viscosity and crystallization behavior when it was compared with properties of the original powder. In the present study, devitrification of industrial basic mold slag sample has been investigated by DTA non-isothermal experiments. Further XRD characterizations give a fairly exhaustive understanding of complex crystallization behavior of mold flux sample under study.

2. Experimental Procedure

The formulated industrial start powder (PF2) for the continuous casting of steel was used in this study. The weight percent composition of the original powder was: humidity (max 0.8%), total carbon (0.5-1.5%), SiO₂ (39-41%), CaO (34.5-36%), Fe₂O₃ (14-16%), Al₂O₃ (2.5-4.5%), Na₂O + K₂O (8-10%), the fluorine as F⁻ (10-12%).

Raw materials and industrial chemical compounds were mechanically mixed with ethanol (same weight as the samples) by rotating mill, equipped with stainless steel grinding system, at rotating speed of 300rpm for 5min. This procedure procured a representative and homogeneous sample of powder avoiding errors due to mass effect. As it can be seen from Figs. 2(a) and (b), by this method the grain size of the samples was comparable to the original start powder (PF2). In Table 1 they are reported the chemical analyses related to prepared mold fluxes which are expressed as weight percentage (normalized to 100 per cent without expressing the loss on ignition).

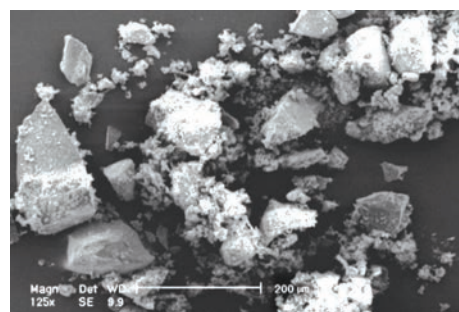
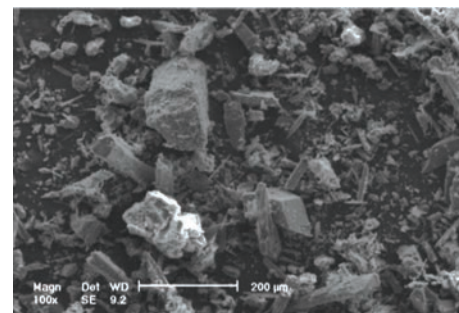


Fig. 2. SEM microstructure of: (a) original start powder (PF2) and (b) H1 clinker base sample.

Table 1. Chemical compositions (in weight percentage %) of prepared mold fluxes.

	SiO ₂	CaO	Fe ₂ O ₃	Al ₂ O ₃	MgO	Na ₂ O	K ₂ O	B ₂ O ₃	TiO ₂	F	S	C
H1	36.02	31.69	13.81	2.11	0.74	8.2	0.29	-	-	4.5	0.002	1.56
H2	35.94	31.63	13.78	2.11	0.74	4.59	0.29	4.49	-	4.49	0.002	0.87
H3	35.98	31.66	13.8	2.11	0.74	0.11	0.29	9.88	-	4.49	0.002	-
E1	34.9	30.71	14.57	4.53	0.91	8.7	0.35	-	-	4.37	0.002	0.98
E2	35.26	31.01	14.71	4.57	0.91	3.72	0.35	5.07	-	4.4	0.002	-
E3	35.61	31.33	14.86	4.62	0.92	6.32	0.36	2.56	-	4.44	0.002	0.5
I1	33.41	29.40	12.81	1.96	0.68	6.77	0.27	-	8.34	4.17	0.002	1.29
I2	34.89	30.68	13.37	2.05	0.71	7.07	0.28	-	4.35	4.35	0.002	1.35
I3	35.80	31.50	13.73	2.10	0.73	7.26	0.29	-	1.79	4.47	0.002	1.39
J1	32.93	28.97	12.92	4.27	0.85	6.76	0.33	-	8.22	4.11	0.002	0.63
J2	34.34	30.21	13.47	4.46	0.89	7.05	0.34	-	4.29	4.29	0.002	0.66
J3	35.24	31.01	13.83	4.57	0.91	7.24	0.35	-	1.76	4.40	0.002	0.68

2.1. Viscosity measurements

The high temperature viscosity of liquid mold flux was measured by a groove viscometer on a 45° slope. In this method the viscosity of mold powders can be measured differentially. The equipment is shown in Fig. 3. About 1g of each sample was used for pressing and producing disk shape specimens with 2mm in height and 13mm in diameter. After the specimens were placed on top of the viscometer, the set was heated up to 1423 K and then it cooled in the furnace.



Fig. 3. Groove viscometer for measuring and comparing the viscosity of the samples.

2.2. Quenched slag preparation

The crystallization of liquid mold fluxes is simpler than the crystallization of glassy mold fluxes. On the other hand, it needs to overcome a potential barrier, i.e. the activation energy E . Thus a glass piece was prepared in order to compare the mold powder free of contaminants and the reference start powder PF2. The powder was placed in an Alumina crucible in the furnace at 1523 K for 7 minutes which represents

the minimum period of time necessary to complete melting of material. The quenching apparatus was constituted of a home designed couple of copper plates 4 mm in height and 400 mm in width. The molten slag batches at 1523 K were extracted from the furnace and rapidly poured on to the first copper plate and immediately squeezed with the another one. In this way, it was realized the fast quenching of molten slag to room temperature. A few minutes later, it was possible to find a layer of glassy material divided into small pieces with a thickness of about 1 mm. These various fragments of glassy material, having different sizes, were recovered and milled to get fine powder with the average dimensions of particle under 100 μm . The Samples with 20 mg weight were analyzed in a differential thermal analyzer (DTA) at a heating rate of 20°C/min in a platinum pan using alumina as the reference material. Heat treatment of samples at 1573 K was performed in the same furnace in an Alumina crucible.

Induced crystallization of the initially vitreous samples was taken into account when the analysis of the crystalline phases is investigated by XRD. For this purpose, the samples were heated up to 1173 K and then cooled in the furnace to partial crystallization. This temperature is higher than the maximum crystallization temperature observed by DTA for all the samples.

3. Results and discussion

Experiments were carried out on the industrial start powder (PF2) which is used in the continuous casting of steel unit in Mobarakeh steel complex (Iran) and low fluorine samples prepared in this study. Phases such as wollastonite, fluorite, silica, alumina and hematite were observed in PF2 powder. Fig. 4 shows the XRD pattern of this powder.

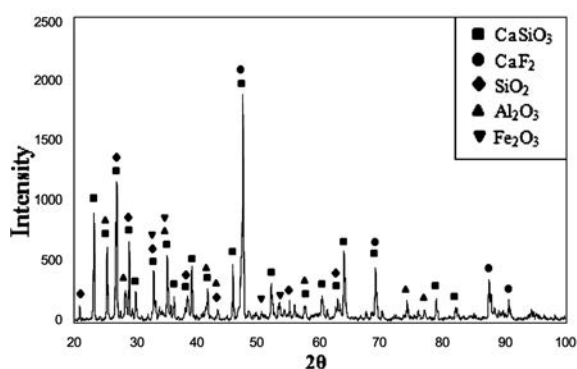
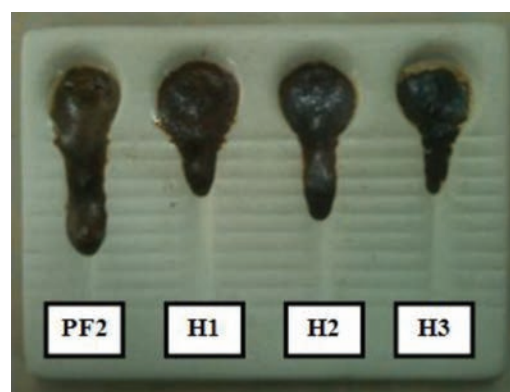


Fig. 4. XRD pattern of PF2 start powder.

In this study 12 specimens were prepared by low fluorine powder. Their chemical compositions were chosen considering Na_2CO_3 , B_2O_3 , TiO_2 and lower fluorine contents. The base composition from cement clinker is very similar to the original start powder. Na_2CO_3 was added as a source of Na_2O and calcium fluoride and cryolite were used as a source of F^- , and the other compositions were achieved by adding the pure oxides.

In the first group, using calcium fluoride, the fluorine content was decreased from 10-12wt% in the original start powder to about 5wt% then it was characterized the effect of replacing Na_2CO_3 and B_2O_3 . Figs. 5(a) shows the influence of these parameters on the viscosity of samples in group 1 compare to the original start powder. As it can be seen, the viscosity increases with decreasing the fluorine content (calcium fluoride) and in the H3 sample, a partial melting was occurred as a result of the rapid melting of B_2O_3 . In the H1 sample, considering the high viscosity, sample melting was much more uniform. In this case, samples of the second group were prepared by the similar compositions but cryolite was used as a source for F^- . Fig. 5(b) shows that the cryolite acts better than calcium fluoride in decreasing the viscosity. The results show that the H1 sample with about 5wt% fluorine and exceeded Na_2O content has the viscosity same as the original powder with 10wt% F^- . Some variations in the viscosity of the sample PF2 in two Figs. 5(a) and (b) is caused by temperature deviations of the furnace, so that the comparison of viscosity of H1 sample with PF2 has been performed in each viscometer independently. DTA experiments were conducted as described in previous section at the heating rate of 20 K/min on the glassy samples which had been prepared with cooling plates method. In DTA measurements it has been pointed out to the complex devitrification nature of these samples. As it can be seen in Fig. 6, there isn't any exothermic peak in DTA results for E1 sample. This phenomenon can be the result of both low fluorine content and presence of cryolite as a source for F^- instead of calcium fluoride. The cryolite is a glass former and the formation of cuspidine

cannot be happen. So in this case, considering the strong influence of cryolite to decrease the viscosity, calcium fluoride needs to be used for the formation of cuspidine and so to approach the optimum crystal fraction for this powder. In addition, calcium fluoride can be replaced with some other components that can produce a crystalline phase or at least encourage the formation of cuspidine crystal phase.



(a)



(b)

Fig. 5. Photo of viscosity measurements using groove viscometer on a 45° slope for (a) samples in group H and (b) samples in group E.

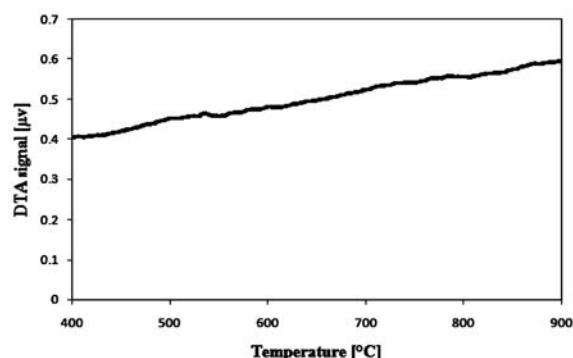
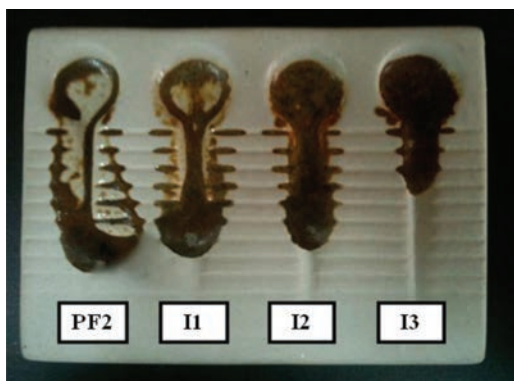


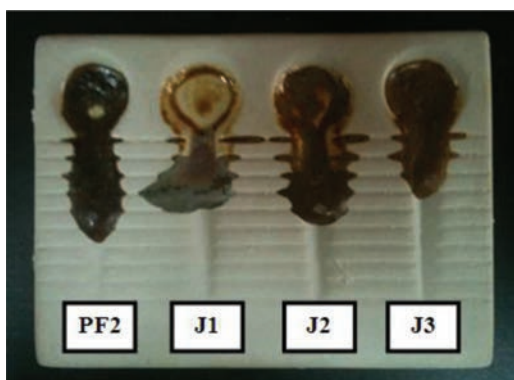
Fig. 6. DTA of E1 sample.

For this purpose, TiO_2 was chosen to produce perovskite (calcium titanium oxide) and subsequently therefore the proper crystal fraction can be achieved.

Thus TiO_2 , as a crystal former, was added about 8, 5, 2wt% to the third and fourth groups. The difference between these samples is using calcium fluoride in group 3 and cryolite in group 4. Figs 7(a) and (b) show that titanium dioxide, with these amounts, acts as a network breaker and decreases the viscosity by itself. The sample I1 with about 8wt % TiO_2 and 4.5wt% F⁻ in group 3 and the sample J2 with 5wt% TiO_2 and same F⁻ content in group 4, had the viscosity similar to the original start powder with 11wt% F⁻.



(a)



(b)

Fig. 7. Photo of viscosity measurements using groove viscometer on a 45° slope for (a) samples in group I and (b) samples in group J.

Figs 8 and 9 show DTA results related to the low fluorine powders of PF2 and I1. As it can be seen in the original start powder, the well defined exothermic peak suggests the crystallization of one crystal phase so that it is detected as cuspidine phase in further XRD analyses (Fig.10). In sample I1, the formation of three different crystalline phases is determined by three exothermic peaks. The XRD investigations of heat treated glassy specimens, which had been produced from cooling disks method, showed the crystallization of three phases, namely perovskite (CaTiO_3), calcium fluoride silicate ($\text{Ca}_{5.75}\text{Si}_2\text{O}_{9.5}\text{F}_{0.5}$) and cuspidine ($\text{Ca}_4\text{F}_2\text{Si}_2\text{O}_7$) (Fig.11). The Comparison of cuspidine peaks from sample I1 with the original start powder showed that they are weaker in the

original powder; It can be concluded that decreasing CaF_2 content to about 4.5wt%, the crystallization of cuspidine becomes more difficult and instead of it, calcium fluoride silicate with lower content of fluorine crystallizes. Another crystalline phase was perovskite which have been observed for sample I1. The observed Crystalline phases effectively have been related to peaks measured in DTA experiments due to the remarkable consistency of crystallization temperature from DTA and XRD measurements. It can be concluded that P^I corresponds to the crystallization of calcium fluoride silicate phase, while P^{II} and P^{III} are two peaks related to the crystallization of cuspidine and perovskite phases respectively.

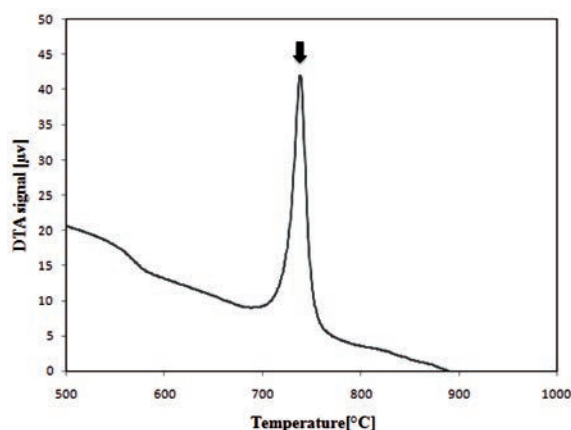


Fig. 8. DTA of PF2 original start powder.

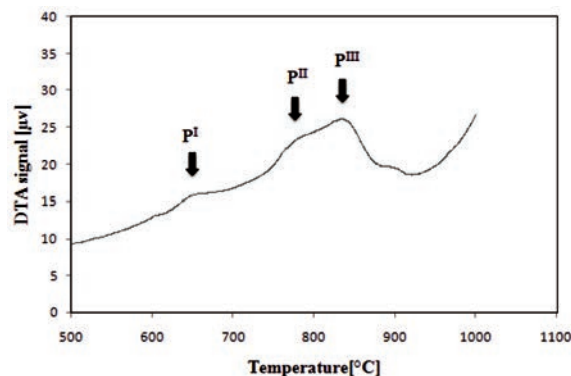


Fig. 9. DTA of I1 sample.

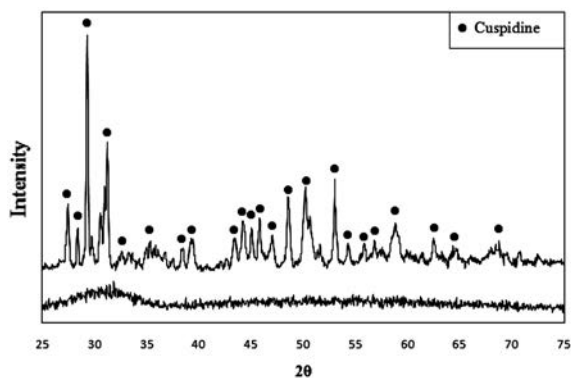


Fig. 10. XRD pattern of PF2 original start powder.

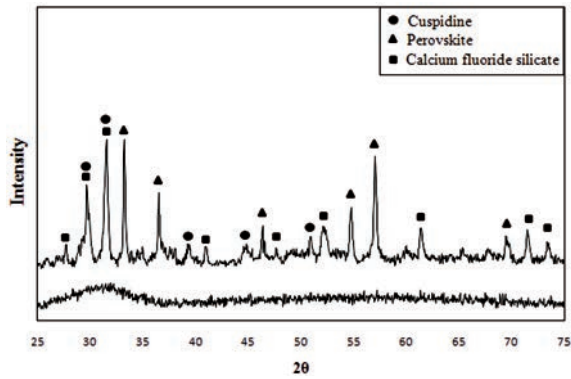


Fig. 11. XRD pattern of I1 clinker based sample.

In powder J2, DTA measurements show only two weak peaks (Fig.12) and XRD investigations show two crystalline phases of calcium fluoride silicate and perovskite, but there was no cuspidine (Fig.13). This phenomenon could be due to the presence of cryolite instead of calcium fluoride in this sample. Because of glass forming nature of cryolite, low amount of F and lack of free CaF_2 , the formation of cuspidine is not remarkable thus it is not detectable by XRD. As a result, P^I corresponds to the crystallization of calcium fluoride silicate and P^{II} relates to perovskite.

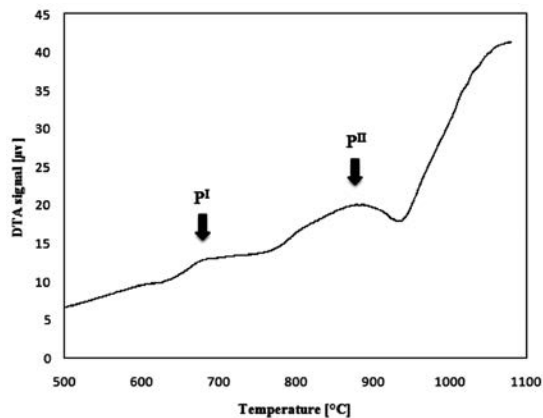


Fig. 12. DTA of J2 sample.

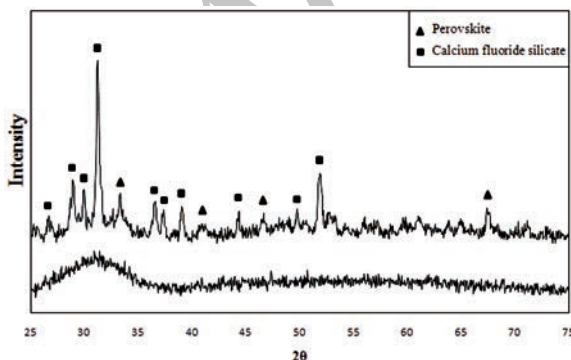


Fig. 13. XRD pattern of J2 clinker based sample.

As far as total amounts of crystalline phases which are practically formed is concerned, crystal fractions has been evaluated through Riaz method⁽²⁰⁾ and XRD patterns:

$$\text{Crystals in slag film\%} = 100 \times \left[\frac{\text{area under peaks}}{\text{total area}} \right]$$

Table 2 shows the amounts of crystal fractions. As it can be seen, this value for the original start powder and the sample I1 is similar and between 40-50%, but it is much lower for the sample J2. From the above analysis, it can clearly be seen that TiO_2 strengthens the crystallization capacity of mold fluxes. In addition, changing TiO_2 content, the type and amount of crystalline phases also will be differed. Increasing in TiO_2 content, the precipitated crystals will change from cuspidine to perovskite.

Table 2. Crystal fraction of PF2, I1 and J2 samples.

Sample	PF2	I1	J2
Crystallinity	46.39	41.06	16.07

4. Conclusion

- CaF_2 in the mold powder can be replaced to some extent by a combination of TiO_2 and Na_2CO_3 .
- Using Na_2CO_3 and B_2O_3 , It was achieved a viscosity equal to the viscosity of the industrial mold powder containing CaF_2 , but Na_2CO_3 produces a more uniform glassy phase.
- The nearly similar amount of crystallinity in the solidified slag in the reference powder (PF2), which influences heat transfer of the solidifying steel shell to the mold, can be obtained by addition of TiO_2 which nucleates the phase formation of CaTiO_3 .
- Increasing TiO_2 content, it also increases crystallization ratio of slag film. When TiO_2 content is about 5%, the precipitated crystal is mainly cuspidine and calcium fluoride silicate; when the TiO_2 content is higher than 8%, the crystal precipitated from slag film is mainly perovskite.
- It has been shown that the cryolite is much more effective than calcium fluoride in decreasing the viscosity, but it has destructive influence on crystallization of cuspidine phase.
- As a result, increasing TiO_2 content, it is enhanced crystallization capacity of the slag. Moreover, the difference in TiO_2 contents will lead to a difference in mineral phase structure. Increasing TiO_2 content, the precipitated crystal will turn from cuspidine into perovskite. DTA and XRD studies in the new system showed that, three phases are developed which are perovskite (CaTiO_3), Calcium Fluoride Silicate ($\text{Ca}_{5.75}\text{Si}_2\text{O}_{9.5}\text{F}_{0.5}$) and Cuspidine ($\text{Ca}_4\text{F}_2\text{Si}_2\text{O}_7$).

5. References

- [1] R.W. Soares, M.V.A. Fonseca, R. Neuman, V.J. Menezes, A.O. Lavinhas and J. Dweck: *Thermochim. Acta*, 318 (1998), 131.
- [2] Y. Meng and B.G. Thomas: *Metall. Mater. Trans. B*, 34(2003), 707.

- [3] X. Qi, G.H. Wen and P. Tang, *J. Non-Cryst. Solids.*, 354 (2008), 5444.
- [4] G. Wen, S. Sridhar, P. Tang, X. Qi and Y. Liu: *ISIJ Int.*, 47 (2007), 1117.
- [5] A.B. Fox, K.C. Mills, D. Lever, C. Bezerra, C. Valadares, I. Unamuno, J.J. Laraudogoitia and J.Gisby: *ISIJ Int.*, 45(2005), 1051.
- [6] N.C. Machingawuta, S. Bagha and P. Grieveson: *Steelmaking Conference Proceedings*, Washington, D.C., 74(1991), 163.
- [7] T. Cimarelli: *Metall. Ital. Italy*, 89(1997), 31.
- [8] K.C. Mills, S. Sridhar, A.S. Normanton and S.T. Mallaband: *The Brimacombe Memorial Symposium*, Vancouver, (2000), 781.
- [9] J. Cho, H. Shibata, T. Emi and M. Suzuki: *ISIJ Int.* 38(1998), 440.
- [10] K.W. Yi, Y.T. Kim and D.Y. Kim, *Met. Mater. Int.*, 13 (2007), 223.
- [11] S.Y. Choi, D.H. Lee, D.W. Shin, J.W. Cho and J.M. Park: *Journal of Non-Crystalline Solids*, 345&346 (2004), 157.
- [12] A. Yamauchi, K. Sorimachi and T. Yamauchi: *Ironmak. Steelmak.*, 29(2002), 203.
- [13] D.T. Stone and B.G. Thomas: *Canadian Metallurgical Quarterly*, Netherlands, 38(1999), 363.
- [14] R. Carli and C. Righi: 7th International Conference on Molten Slags Fluxes and Salts, The South African Institute of Mining and Metallurgy, (2004), 821.
- [15] K.C. Mills, A.B. Fox, R.P. Thackray and Z. Li: 7th International Conference on Molten Slags Fluxes and Salts, The South African Institute of Mining and Metallurgy, (2004).
- [16] R. Taylor and K.C. Mills: *Ironmak. Steelmak.* 15 (1988), 187.
- [17] T. Watanabe, H. Fukuyama and K. Nagata, *ISIJ Int.*, 42 (2002), 489.
- [18] C. Righi, R. Carli and V. Ghilardi: *Proceedings 6th International Conference on Molten Slags Fluxes and Salts*, Stockholm Helsinki, (2000).
- [19] M.L. Koul, S. Sankaranarayanan, D. Apelian and W.L. McCaulery, *Press of Northeast University of Technology*, (1988), 2.
- [20] K.C. Mills, L. Courtney, A.B. Fox, B. Harris, Z. Idoyaga and M.J. Richardson: *Thermochim. Acta*, 391 (2002), 175.

Archive of SID

SID



سرویس های
ویژه



سرویس ترجمه
تخصصی



کارگاه های
آموزشی



بلاگ
مرکز اطلاعات علمی



عضویت در
خبرنامه



فیلم های
آموزشی

کارگاه های آموزشی مرکز اطلاعات علمی جهاد دانشگاهی



مباحث پیشرفته یادگیری عمیق؛
شبکه های توجه گرافی
(Graph Attention Networks)



کارگاه آنلاین آموزش استفاده از
وب آوساینس



کارگاه آنلاین مقاله روزمره انگلیسی